Electronic excitation by electron impact of the O2 molecule physisorbed on a metal

B. Bahrim, D. TeilletBilly, and J. P. Gauyacq

Citation: The Journal of Chemical Physics **104**, 10014 (1996); doi: 10.1063/1.471746
View online: http://dx.doi.org/10.1063/1.471746
View Table of Contents: http://scitation.aip.org/content/aip/journal/jcp/104/24?ver=pdfcov
Published by the AIP Publishing

Electronic excitation by electron impact of the O_2 molecule physisorbed on a metal

B. Bahrim,[a] D. Teillet-Billy, and J. P. Gauyacq[b]
Laboratoire des Collisions Atomiques et Moléculaires, Unité de Recherches Associée au CNRS 281, Université de Paris-Sud, Bât, 351, 91405 Orsay Cedex, France

(Received 13 February 1996; accepted 22 March 1996)

The electronic excitation process by low energy electron impact is studied theoretically for the case of O_2 molecules physisorbed on a model jellium metal (Al). The spin forbidden excitations to the $a\ ^1\Delta_g$ and $b\ ^1\Sigma_g^+$ states are considered. Only the resonant contribution corresponding to the $^2\Pi_g\ O_2^-$ resonance, which dominates at low energy in the free molecule is included in the present work. The characteristics of this resonant process involving a resonant state hidden below the excitation threshold are analyzed; in contrast with the free molecule case, a very important excitation process occurs below the energy threshold. The dependence of the excitation process on the symmetries of the problem is also discussed. © *1996 American Institute of Physics.* [S0021-9606(96)02124-1]

I. INTRODUCTION

The excitation of spin-forbidden transitions by electron impact on small diatomic molecules requires an exchange process i.e. a process in which the incident and outgoing electrons are in different spin states. For free molecules, such transitions have indeed be observed in a variety of systems and are associated with sizable cross sections close to threshold.[1] The oxygen molecule is a good example of this, it presents both a fundamental interest because of its open shell electronic structure and a practical interest because of the large number of physical situations in which it is present. For the free molecule, rather strong electronic excitation from the ground state ($X\ ^3\Sigma_g^-$) to the first two excited states ($a\ ^1\Delta_g, b\ ^1\Sigma_g^+$) have been observed from threshold up to a few tens of eV.[2–6] Resonant mechanisms have been shown to quantitatively account for the main features of this excitation processes at low energy.[7–10] The most important one, responsible for the bulk of the low energy excitation cross section involves the $O_2^-(^2\Pi_g)$ resonance; it is associated to the $(1\pi_u^4\ 1\pi_g^3)$ electronic configuration and is formed by adding a π_g electron in the partly filled $1\pi_g$ shell of the neutral O_2 molecule fundamental configuration $(1\pi_u^4\ 1\pi_g^2)$. It is noteworthy that three states are associated to the $(1\pi_u^4\ 1\pi_g^2)$ configuration; the ground $X\ ^3\Sigma_g^-$ state and the two excited $a\ ^1\Delta_g$ and $b\ ^1\Sigma_g^+$ states; thus, the $O_2^-(^2\Pi_g)$ resonance appears as a link between the X, a, and b states and thus it provides an easy way to excite the O_2 molecule from the X to the a and b states.

Resonant processes have been shown to be very efficient intermediates in the excitation of free molecules by low energy electron impact[11] and the same feature was also found in the case of adsorbed molecules.[12,13] This subject is now well documented for the case of resonant vibrational excitation of adsorbed molecules; in particular, the resonant vibrational excitation of N_2 molecules physisorbed on metals via the $N_2^-(^2\Pi_g)$ resonance has been studied in detail both experimentally[14–16] and theoretically.[17–23] Resonant processes are usually associated with strong enhancement of the excitation processes in a well defined energy range corresponding to the resonance energy and this is even considered as one of the experimental characteristics required to assign a resonant process. This is for example the case for the $N_2^-(^2\Pi_g)$ resonance both for free and adsorbed molecules.[11,14,21] The situation is quite different in the case of the O_2^- molecule (see discussion in Ref. 8). Indeed, the $O_2^-(^2\Pi_g)$ resonance involved in the a and b excitation is located below the excitation thresholds at the O_2 equilibrium distance and as a consequence the excitation processes cannot maximize at the resonance energy. The resonant excitation cross section in that case displays a rather smooth energy dependence, extending over a large energy range; in this case, the resonant process involves the far wings of the resonance and it appears as a way of recoupling the electronic spin and orbital angular momenta during the collision.

The aim of the present work is to study how such a resonant process, which do not present the usual resonant features for the free molecule, will influence the excitation process in the case of physisorbed molecules. We study O_2 molecules in front of a jellium surface with the Al characteristics, as representative of a physisorption system. The characteristics of the $O_2^-(^2\Pi_g)$ resonance (energy position and lifetime) interacting with an Al surface have already been determined;[24] here, we concentrate on the dynamics of the resonant energy transfer, i.e., to the resonant excitation from the ground state to the a and b states of O_2. After presenting in more details, the $O_2^-(^2\Pi_g)$ resonant excitation process (Sec. II), we will discuss (Sec. III) the symmetry and orientational aspects of the resonant scattering for O_2 physisorbed on a jellium metal (Al). The theoretical method is then presented in Sec. IV and results and discussion of the process are presented in the last section with emphasis on the angular symmetry aspects associated with the adsorption geometry.

Electronic excitation of adsorbed molecules has been the subject of many experimental works which showed the im-

[a]Also at: Atomic Physics Institute, IFTAR, Laser Department, P.O. Box MG-6, Bucarest Magurele, Romania.
[b]Corresponding author; electronic mail: gauyacq@lcam.u-psud.fr

 0021-9606/96/104(24)/10014/9/$10.00

portance of various resonant processes.[25–27] However, for the O_2 molecule they correspond to collision energies higher than the ones where the O_2^- resonance is dominating. It must be stressed that some experimental studies have been performed on physisorbed systems[27] with a preferential molecular axis orientation (both in polar and azimuth angles) which could lead to the observation of the symmetry effects discussed below.

II. RESONANT EXCITATION OF THE FREE O_2 MOLECULE

The ground state of the O_2 molecule is a triplet state $(1\pi_u^4\ 1\pi_g^2,\ ^3\Sigma_g^-)$ and the excitation of the two singlet states associated to the same electronic configuration, involves an exchange process. The excitation of singlet states by electron impact below 20 eV has been shown to be dominated by resonant processes in particular through the $O_2^-(\pi_g^4\ \pi_u^3)^2\Pi_g$ resonance. In this case, an extra π_g electron is captured by the molecule in its ground state to form the $^2\Pi_g$ intermediate molecular negative ion, that decays by electron emission. It has been shown that the decay channel corresponding to the emission of any of the seven electrons of the O_2^- π shells have to be taken into account.[8] The emission of one of the three π_g electron leaves the molecule in one of the three electronic states associated with the $\pi_u^4\ \pi_g^2$ configuration and in particular in the singlet $a\ ^1\Delta_g$ and $b\ ^1\Sigma_g^+$ excited states under study. The emission of one of the four π_u electrons leaves the molecule in one of the six high lying excited electronic states associated with the $\pi_u^3\ \pi_g^3$ configuration

$$e^- + O_2(1\pi_u^4\ 1\pi_g^2,\ X\ ^3\Sigma_g^-) \rightarrow O_2^-(1\pi_u^4\ 1\pi_g^3,\ ^2\Pi_g)$$
$$\rightarrow e^- + O_2(1\pi_u^4\ 1\pi_g^2,\ X\ ^3\Sigma_g^-,\ a\ ^1\Delta_g,\ b\ ^1\Sigma_g^+)$$
$$\rightarrow e^- + O_2(1\pi_u^3\ 1\pi_g^3).$$

The lowest lying excited states associated with the $(1\pi_u^3\ 1\pi_g^3)$ electronic configuration are around 6 eV above the ground state and so the $1\pi_u$ electron ejection influences the resonance at low energy and has to be considered. This gives a very strong multichannel character to the $O_2^-(^2\Pi_g)$ resonance which can decay into nine different channels.[8] The above resonant scheme is *a priori* rather efficient since it only involves one electron steps; capture of a $1\pi_g$ electron and ejection of a $1\pi_u$ or $1\pi_g$ electron. However, the $O_2^-(^2\Pi_g)$ resonance is located at very low energy, below all the excitation thresholds, this decreases its efficiency since the above excitation processes can only occur in the far wings of the resonance. A more detailed description of this process is presented in Ref. 8. The $(^2\Pi_g)$ resonance process dominates the low energy excitation of O_2. This is illustrated in Fig. 1 which presents the total cross section for the excitation of the a state as a function of the collision energy for free molecules; both experimental[2,3,5] and theoretical results[8,10] are presented. The excitation of the a state appears to be dominated by two resonant processes; excitation via the $O_2^-(^2\Pi_g)$ resonance discussed above and given by the ERT result in Fig. 1 (this calculation only considers the $^2\Pi_g$ intermediate symmetry); excitation via the $O_2^-(1\pi_u^3 1\pi_g^4, ^2\Pi_u)$ resonance

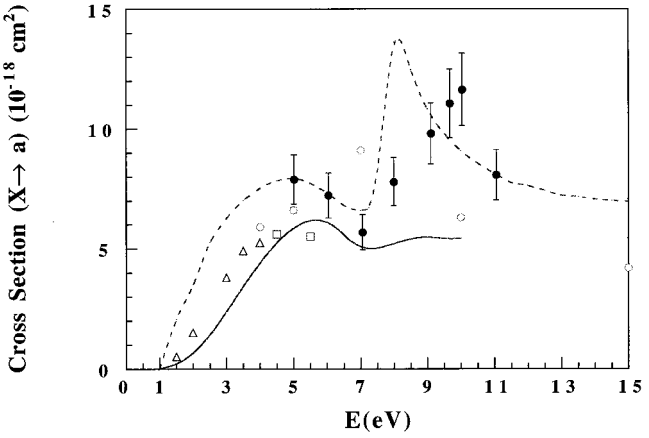

FIG. 1. Total excitation cross section for the $a\ ^1\Delta_g$ state of free O_2 molecules by electron impact as a function of incident electron energy. Full line, ERT results (Ref. 8); dashed line, theoretical results of Noble and Burke (Ref. 10); experiments: triangles, Linder and Schmidt (Ref. 2); open circles, Trajmar *et al.* (Ref. 3), squares, Hall and Trajmar (Ref. 4); full circles with error bars, Middleton *et al.* (Ref. 5).

which appears as a narrow peak around 8 eV in the R-matrix results[10] and around 10 eV in the experimental results of Middleton *et al.*[5]

In the present work, we will concentrate on the $^2\Pi_g$ contribution to this excitation; it appears to yield the bulk of the excitation cross section dominating at low energy on which the $^2\Pi_u$ resonant contribution is superimposed around 10 eV. The shape of the $^2\Pi_g$ excitation cross section does not display the usual resonance shape, it has a rather structureless energy dependence with a $d\pi_g$ threshold law. This is linked to the fact that the $^2\Pi_g$ resonance is hidden below the excitation threshold. The drop around 6 eV in the excitation cross section is due to the opening of the $1\pi_u$ electron ejection processes.

III. MOLECULAR AXIS ORIENTATION AND SYMMETRY

Let us consider the angular description of the $^2\Pi_g$ resonance process and its relation to the molecular axis orientation. In the free molecule, the active $1\pi_g$ electron corresponds to an almost pure $d\pi$ wave in the molecular frame.[28] Both degenerate components of the $d\pi$ wave (Y_{21} and Y_{2-1} spherical harmonics) are involved.

Let us consider now an isolated oriented O_2 molecule adsorbed on a metal surface. The metal surface is considered as a flat surface without any cristallographic structure, as described in the jellium approximation. The symmetry element of this problem, when the molecular axis is not perpendicular to the surface plane ($\beta \neq 0$ in Fig. 2, β is the angle between the molecular axis and the normal to the surface) is the plane normal to the surface and containing the molecular axis. However, if the molecular axis is perpendicular to the surface plane ($\beta = 0$ in Fig. 2) the symmetry plane is transformed into a symmetry axis, the system being invariant by rotation around the molecular axis. So, in the perpendicular geometry, the system retains its molecular symmetry, even if

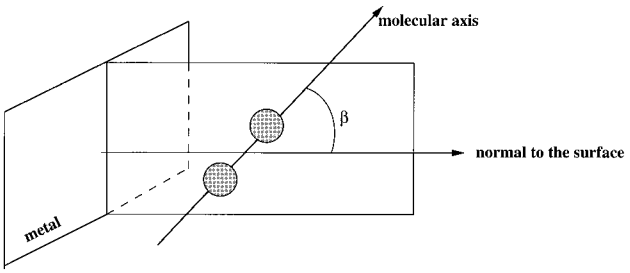

FIG. 2. Schematic diagram of the symmetry elements for the O_2/metal surface system.

the u/g symmetry of O_2 is lost; whereas in nonperpendicular geometries, one has to consider states with a well defined symmetry with respect to the symmetry plane P (see Fig. 2). Indeed, if one wants to explicit the symmetry of the problem, one has to consider symmetry adapted states for the active electron but also for the O_2 target states and for the intermediate O_2^- state. In the following, we will study two different adsorption geometries with the molecular axis either perpendicular or parallel to the surface plane. This study of the two extreme geometries allows a detailed discussion of the molecular axis orientation effect. It has to be considered more as a study of the various geometrical cases than as the study of a precise system; indeed in a real system, the molecule is either parallel or perpendicular. A similar study has already been performed for the case of the $N_2^-(^2\Pi_g)$ resonance, both from a static and dynamic point of view, energy and lifetime of the resonance[29] and vibrational excitation cross sections[23] as functions of the molecular axis orientation. Although both the N_2 and O_2 cases involve a $d\pi$ active electron, the open shell structure of O_2 somewhat modifies the problem.

Let us first consider the symmetry adapted states for the $d\pi$ active electron. At this stage, it is convenient to consider not the spherical harmonics Y_{21} and Y_{2-1}, but rather their sum and difference. The shape of such orbitals is presented in Fig. 3(c) for the perpendicular geometry, one goes from one to the other by a rotation of $\pi/2$ around the molecular axis. Figures 3(a) and 3(b) present the two symmetry adapted orbitals for the parallel geometry. The geometrical shape in both cases resembles that of a cloverleaf; the cloverleaf plane can be either parallel to the surface, this situation corresponding to the symmetric component of the $d\pi$ orbital, or

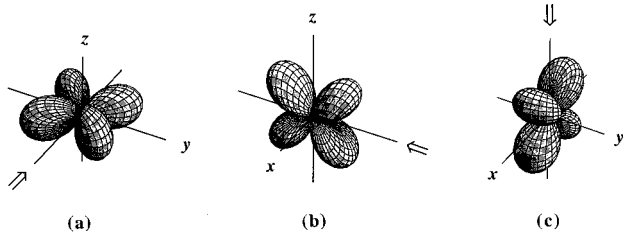

FIG. 3. Shape of the $d\pi$ resonant orbital in the various geometries and symmetries. The surface plane is parallel to the Oxy plane and the molecular axis is indicated by the double arrow. (a) Parallel geometry, antisymmetric component. (b) Parallel geometry, symmetric component. (c) Perpendicular geometry.

either normal to the surface plane, this situation being associated with the antisymmetric component. The interaction with the metal surface lifts the degeneracy of these two components; because of a better overlap a larger interaction is obtained for the symmetric component of the $d\pi$ wave. All these properties can also be understood in terms of rotation matrices. Changing from the molecular frame, where the quantization axis is along the molecular axis to the surface frame, where the quantization axis is along the surface normal, the symmetric (antisymmetric) component of the $d\pi$ orbital corresponds to $l=2$, $m=\pm 1$ ($l=2$,$m=\pm 2$) waves, respectively, in the new frame; this gives rise to an other interpretation for the different interactions of the two components (symmetric or antisymmetric) with the metal surface. The interaction with the metal surface will mix different l values of the angular momentum, leaving the projection of the electron angular momentum into the surface normal unchanged. As a result, the symmetric component will mix, with the $l>2$, $|m|=1$ symmetric components and also with the p, $|m|=1$ symmetric one. The interaction with the metal will be rather large in that case since the mixing with a wave with a smaller centrifugal barrier is allowed. This is not the case for the $l=2$, $|m|=2$, antisymmetric component, which is only mixed with waves with a higher centrifugal barrier, that do not increase the tunneling of the electron.

It is also remarkable from Fig. 3, that the situation of the symmetric component in the parallel geometry is very similar to that of both components of the perpendicular geometry.

Symmetry with respect to the P plane has also to be considered for the O_2 and O_2^- states. The nondegenerate states, $X\ ^3\Sigma_g^-$ and $b\ ^1\Sigma_g^+$, have a well defined symmetry (antisymmetric and symmetric, respectively). The degenerate states $O_2^-(^2\Pi_g)$ and $O_2(a\ ^1\Delta_g)$ splits into two components (symmetric and antisymmetric) in the parallel geometry. If one now considers the entire process, in the perpendicular geometry, the molecular symmetry is preserved; in contrast, in the parallel geometry the symmetric and antisymmetric components (A and S) have to be explicited and behave differently. For example, for the $O_2^-(^2\Pi_g)$ A component,

$$
\begin{aligned}
e^-(S)+O_2(X\ ^3\Sigma_g^-,A) &\rightarrow O_2^-(^2\Pi_g,A)\\
&\rightarrow e^-(A)+O_2(a\ ^1\Delta_g,S)\\
&\rightarrow e^-(S)+O_2(a\ ^1\Delta_g,A)\\
&\rightarrow e^-(A)+O_2(b\ ^1\Sigma_g^+,S).
\end{aligned}
$$

From the above properties of the A and S component of the $d\pi$ orbital, it is possible to discuss the relative importance of the various excitation schemes (see below). As for the width of the two $O_2^-(^2\Pi_g)$ components in the parallel geometry the S active electron being more coupled will lead to a larger width for the A component of the resonance. In addition, the width of the O_2^- A component in the parallel geometry is very close to the O_2^- width in the perpendicular geometry. This accounts for the widths obtained in our previous study.[24] It must be stressed that because of the open shell structure of O_2, the polarization effect in O_2^- (relative value

of the A and S component widths) appears to be inverted as compared to the situation of one electron systems, such as $N_2^-(^2\Pi_g)$.[29]

IV. METHOD

Recently, we have proposed a new nonperturbative method to treat resonant electron scattering by molecules adsorbed on a metal surface.[19,21–23,30] The basic idea of this method named coupled angular mode (CAM) method[31] is to study the electron scattering by a compound interaction formed by the superposition of the electron molecule and electron–surface interactions. They are supposed not to be perturbed one by the other and for this reason, the applicability of the method is restricted to physisorbed systems. In this method, the metal is described as a jellium, i.e., without a crystallographic structure. Recently, studies of negative molecular ion–metal surface systems at the static level[32] (determination of resonance energies and widths) showed that the crystallographic structure of the surface acting via the surface reflectivity could influence the resonance characteristics. It was found that this was the case for the higher lying resonances; however, low lying resonances, such as the $N_2^-(^2\Pi_g)$ resonance located around 2 eV, was not much influenced by the crystallographic structure. Here, the $O_2^-(^2\Pi_g)$ resonance is very low lying (around zero for the free molecule) and in the present approach, the leading term of the influence of the surface on the resonance is the electrical image interaction. The CAM method has first been applied to the static study of the properties of the molecular negative ion resonance formed in the scattering process. In that case, molecular resonance with fixed internuclear distances are considered; molecular negative ions appear as a resonant feature in the electron scattering process and can be further analyzed. Both energy position and detachment width can be consistently extracted from the calculation of the scattering S matrix. Inelastic electron scattering can be handled by this method when the excitation channels are included in the theoretical development. Recently, the method has been extented to handle vibrational excitation of the adsorbed molecule as resonantly induced by electron impact. We propose here a further extension of the method to treat the electronic excitation problem. It is noteworthy that this extension is the same as the one we used previously to treat the multielectron multistate effects in the O–Al charge transfer process during a collision.[24,33,34]

A. Electron–surface interaction

The electron–surface interaction is described in the jellium approximation. It is considered as a local potential only function of z, the electron–surface distance. We used the potential given by Jennings, Jones, and Weinert,[35]

$$V_s = -\frac{1}{4z}\left[1-\exp(-\lambda z)\right] \quad z>0,$$

$$V_s = -U_0/(1+A\ \exp\ Bz) \quad z<0, \tag{1}$$

where $z>0$ corresponds to the vacuum side. λ and U_0 are parameters depending in the free electron metal. We have considered an Al surface. However, as previously discussed,[19] the properties of the negative ion systems do not depend too much on the free electron metal characteristics as long as the resonant state is not located near the bottom of the metal conduction band. In formula (1), the distance is measured from the image reference plane; below, the distances between the molecule and the surface are also measured from this plane.

B. Electron–molecule interaction

The electron O_2 molecule interaction is modeled in the effective range theory approximation (ERT). We make use of the multielectron, multistate version of this approach that has been developed to treat the electronic excitation of free O_2 molecules by electron impact.[8] A detailed description can be found in Ref. 8. The basic idea of the ERT approach is to cut the space for the collisional electron in two regions;

(a) An outer region, where all channels are decoupled and where the electron interacts with the molecule via a local potential which retains the spherical symmetry;
(b) An inner region, where the electron–molecule interaction is complex and in which the system wavefunction is assumed to be independent of the collision energy. The solution of the collision problem is then obtained by matching for each symmetry (i.e., each angular momentum) the energy independent solution of the inner region to the solution in the outer region. This matching is performed at a distance $r=r_c$ from the molecule.

In the case of the O_2 molecule, for the symmetries of the total system different from $^2\Pi_g$ and $^2\Pi_u$, one can use the one electron version of the ERT which reduces to a boundary condition on the outer region electron wave function at the boundary between the two regions [$r=r_c$ (see, e.g., our study of e^--N_2 collisions)]. For the nonresonant symmetries, these boundary conditions were adjusted to reproduce phase shifts for a polarization potential.[36]

For the $d\pi$ symmetry of the collisional electron, one has to consider the $(^2\Pi_g)O_2^-$ resonance which involves multielectron and multistate effects. In that case, the wave function of the e^--O_2 system in the inner region is assumed to be the $O_2^-(^2\Pi_g)$ resonant wave function described as a Slater determinant, $|1\pi_u^4\ 1\pi_g^3|$ (the inner electrons are not indicated). This Slater determinant can be expanded with respect to its lines or its columns to yield a superposition of products of one electron wave functions by O_2 states wave functions. The O_2 states included are the three states associated with the $(1\pi_u^4\ 1\pi_g^2)$ configuration and the six states associated with the $1\pi_u^3\ 1\pi_g^3$ configuration. The expansion is very easily matched on the boundary to a close coupling expansion in the outer region, i.e., to a superposition of products of O_2 states by the scattering electron wave functions. All the quantities required for this description have been extracted from an *ab initio* study of the e^--O_2 system.[8]

In the $^2\Pi_u$ symmetry (incident $p\pi$ electron), O_2 presents the well known $^2\Pi_u$ resonance associated with the configuration $(1\pi_u^3\ 1\pi_g^4)$ (see Sec. II). In the present work, this reso-

nant state was not fully introduced. However, since its description requires the knowledge of the $1\pi_u$ and $1\pi_g$ molecular orbitals, assuming that these orbitals are the same as in the $^2\Pi_g$ resonant state can provide the ERT boundary condition for the $^2\Pi_u$ state. This has been done in the present work and the $^2\Pi_u$ resonance appears around 7 eV in the free molecule with the above assumptions. However this resonance is only introduced in the $(1\pi_u^3\ 1\pi_g^3)$ channels and its decay in the X, a, and b channels which involves two electron transitions has not been introduced and so, the contribution to the electronic excitation of the a and b states via this resonance is not included in the present study.

C. CAM collision equations

The e^-–surface and e^-–molecule interactions have quite different symmetry properties. In the CAM approach we use an approach that favors the molecular symmetry; we describe the electron scattering wavefunction by an expansion over spherical harmonics, that is to say we develop the electron wave function in the angular eigenmode of the electron–molecule scattering. As a result, when considering the compound molecule+metal surface, the electron–metal surface interaction couples these angular eigenmodes. The total wave function for the collisional system in the outer ERT region is written as

$$|\Psi\rangle = \sum_{\lambda} \sum_{l,m} \frac{1}{r} Y_{lm}(\theta,\varphi) F_{lm}^{\lambda}(r) |\phi_{\lambda}\rangle, \tag{2}$$

where Y_{lm} are spherical harmonics centered on the molecule center with the z axis normal to the surface, ϕ_λ are the electronic states of O_2 introduced in the calculations (all the states associated with the $1\pi_u^4\ 1\pi_g^2$ and $1\pi_u^3\ 1\pi_g^3$ configurations), and $F_{lm}^{\lambda}(r)$ is the radial wave function for the collisional electron in the (λ,lm) channel. Expansion (2) is brought into the Schrödinger equation to yield coupled equations for the F_{lm}^{λ}. Since in the outer region the electron is interacting with the molecule via a local potential, these equations are block diagonal in λ and the $F_{lm}^{\lambda}(r)$ are only coupled inside a given λ block by the electron–surface interaction. At the ERT boundary, expansion (2) must match the wave function in the inner region, this is done via the ERT boundary conditions (see above and in Ref. 8 for more details).

Expansion (2) does note take into account the vibrational motion of the molecule i.e., it corresponds to a calculation performed at fixed internuclear distance R. In the following, the calculations are performed for the O_2 equilibrium distance. This procedure makes the implicit assumption that, on the scale of the collision time, the two atoms do not move. This assumption will be further discussed below.

The symmetry is different in the perpendicular and parallel geometries and this has to be reflected in the collision equations. In the perpendicular geometry, m is a good quantum number and in expansion (2) one only has to retain the $(m=\pm 1)$ terms corresponding to the $O_2^-(^2\Pi_g)$ resonance symmetry. Indeed, the u/g symmetry is lost and all l values $(l \geqslant 1)$ are coupled. In the parallel geometry, the molecular symmetry is lost and m is no more a good quantum number. However, in the outer ERT region where the coupled equations are solved, the coupled equations are block diagonal in m and λ (the coupling between different m and different λ terms is introduced by the ERT boundary condition). So, in the parallel geometry, the problem is solved in two steps; first, the ERT boundary condition for the radial wavefunction is used in the *molecular frame* to start the solutions, then by rotation these solutions are brought into the *surface frame* [the one used in expansion (2)] and the coupled equations are solved in this frame. The calculation is performed twice, one for each symmetry of the intermediate O_2^- state (symmetric or antisymmetric state with respect to the plane P in Fig. 2). In both geometries, the propagation is performed up to a large distance $r=r_{\mathrm{Max}}$, where the scattering S matrix is extracted. In fact, at large r, the spherical harmonics are still coupled by the e^-–surface interaction and the S matrix is extracted in the adiabatic angular basis (see Refs. 31, 22).

At this stage of the calculation, two different kinds of information can be obtained; either the characteristics of the resonant state (position and lifetime) via the analysis of the time delay matrix (this has been performed on O_2 in Ref. 24), or the excitation cross sections and probabilities and this is the subject of the present work.

D. Inelasticities and excitation cross sections

The angular expansion used in our calculation is not enough to provide converged angular distributions for the various inelastic processes. However, it provides converged results for the total excitations. The situation encountered for electronic excitation is very similar to that encountered in our previous study of the vibrational excitation process[22] and we used the same methods. First, we define the inelasticity for each excitations as

$$I_{\lambda\to\lambda'} = \sum_{i,j} |S_{ij}^{\lambda\to\lambda'}|^2, \tag{3}$$

where $\lambda(\lambda')$ is the index for the initial (final) state of the studied excitation process, i and j are indices for the adiabatic angular modes used for the extraction of the S matrix.

The inelasticity can be considered as an excitation probability. For the free molecule, the inelasticity is directly linked to the total excitation cross section,

$$\sigma_{\lambda\to\lambda'}^{\mathrm{Tot}} = \frac{\pi}{k_\lambda^2}\, \alpha I_{\lambda\to\lambda'}, \tag{4}$$

where k_λ is the wave number in the incident channel, α is a statistical factor (2/3) in the present case for the $O_2^-\ ^2\Pi_g$ resonant intermediate, and for excitations from the O_2 ground state.

In the case of a target molecule adsorbed on a metal surface, the space around the molecule is not isotropic anymore and the situation is physically very different if, for example, the electron is scattered into the metal or into the vacuum. To stress this point we define four different ''summed cross sections'' as the integral over the final angle and the average over the initial angle of the differential cross

sections; the integration and average are restricted to the half space corresponding to the vacuum or to the metal side.

The four summed cross sections are then σ_{VV}, the incident and scattered electrons are in the vacuum, this corresponds to the usual scattering experiment; σ_{VM}, the electron comes from the vacuum and is scattered into the metal; this process is present in a usual scattering experiment, however it is not observed; σ_{MV} and σ_{MM} correspond to the situations with an electron coming from the metal side. The corresponding experiments involve hot electrons or photoelectrons.

In our previous study of vibrational excitation of N_2, we derived two different methods to compute the summed cross sections, the predictions of which were found in good agreement with each other. Here we only used the classical method, which evaluates the summed cross sections from the inelasticities via classical angular sharing factors (see Ref. 22). They are defined as (for the excitation process from state λ to state λ')

$$\sigma_{AB}^{\lambda\to\lambda'}=\frac{\pi}{k_\lambda^2}\,\alpha I_{\lambda\to\lambda'} g_A g_B, \tag{5}$$

where k_λ is the wave number for the incident electron, α is a statistical factor, A,B stands for V or M, g_A and g_B are the angular sharing factors. The factor g_V factor is obtained as the probability that an electron emitted from the molecule center according to the unperturbed resonant orbital angular shape ($d\pi$ wave in the present case) can overcome the surface barrier and escape into the vacuum. g_M is equal to $(1-g_V)$. These factors depend on the electron energy and on the polarization of the resonance; they concern both the incident and outgoing electrons.

V. RESULTS AND DISCUSSION

A. Resonance characteristics

Let us first recall the results of Ref. 24 on the position and width of the $O_2^-(^2\Pi_g)$ resonance when adsorbed on a model Al surface. For the adsorption height of 5 a_0, studied here, the resonance is located around $(-1.34$ eV), i.e., below vacuum, with a very small dependence on the geometry and symmetry. The width in contrast depends much on the symmetry, it amounts to around 0.14 eV in the perpendicular geometry and for the antisymmetric component in the parallel geometry and it amounts to around 0.07 eV for the symmetric component in the parallel geometry. These symmetry differences can be very well accounted for by comparing the various relative positions of the resonance orbital and of the metal surface (see Fig. 3 and Ref. 29).

B. Inelasticities

Figures 4(a) and 4(b) present the inelasticities for the excitation from the O_2 ground state to the $a\ ^1\Delta_g$ and $b\ ^1\Sigma_g^+$ states as functions of the incident energy. As mentioned above, only the resonant contributions due to the $O_2^-(^2\Pi_g)$ resonance are included. The electron energy is referred to the vacuum level. Figure 4(a) presents the case of a molecule

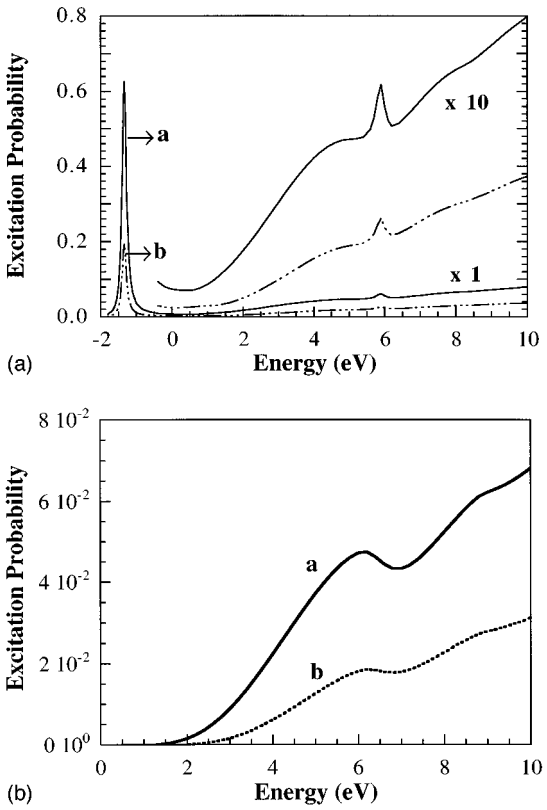

FIG. 4. (a) Excitation probabilities for the a and b states of the O_2 molecule adsorbed in the perpendicular geometry as functions of the incident electron energy. Full line, excitation to the $a\ ^1\Delta_g$ state. Dashed–triple dotted line, excitation to the $b\ ^1\Sigma_g^+$ state. (b) Same as (a) for the free molecule. Full line, excitation to the $a\ ^1\Delta_g$ state. Dotted line, excitation to the $b\ ^1\Sigma_g^+$ state.

adsorbed in the perpendicular geometry at a distance of 5 a_0 from the surface (measured from the image reference plane). This distance has been chosen as representative of typical physisorption distances. It is compared [Fig. 4(b)] with the results for a free molecule (taken from Ref. 8). The inelasticities in Fig. 4(a) present two regions with different behaviors.

First for positive energies, the inelasticity increases with the collision energy in a way very similar to that of the free molecule, except for an energy shift. This is a rather remarkable feature; the resonant process appears not to be much modified although the resonance has been shifted by more than 1 eV and the resonance width has increased from 0.25 meV to around 0.1 eV. The interpretation of this region parallels that for the free molecule (see Ref. 8). In the resonant process, the incident electron is captured to form an O_2^- transient ion which later decays leaving the molecule excited. However, in the few eV range, capture of the incident electron barely occurs since the electron energy is well above the centrifugal barrier both in the incident and outgoing channels; the excitation probability then depends on the values of incident and outgoing fluxes and on the fractional parentage coefficients[37] which give the weight of each electronic channel in the resonant wave function [see, for example, the discussion in $(e^-$-O)]. Except for an energy shift due to image forces, these characteristics are not much influenced by the

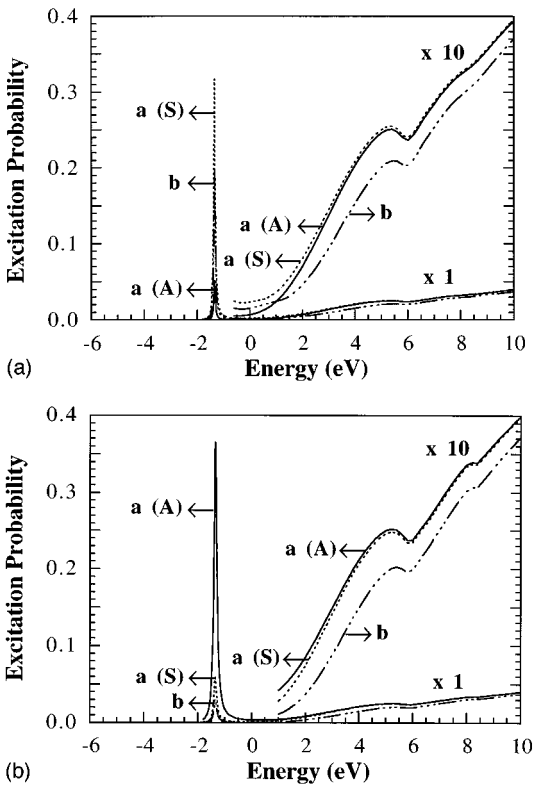

FIG. 5. (a) Excitation probabilities of the O_2 molecule adsorbed in the parallel geometry as functions of the incident electron energy (symmetric component of the O_2^- resonant intermediate). Dashed line, excitation of the symmetric component of the $a\ ^1\Delta_g$ state. Full line, excitation of the antisymmetric component of the $a\ ^1\Delta_g$ state. Dashed–triple dotted line, excitation of the $b\ ^1\Sigma_g^+$ state. (b) Same as (a) for the antisymmetric component of the O_2^- resonant intermediate.

adsorption. In Fig. 4(a), the peak around 6 eV must be considered as an artefact; it is due to the $O_2^-(^2\Pi_u)$ resonant state, however, due to its uncomplete description in the present study, the peak cannot be considered as an estimate of the $^2\Pi_u$ contribution to the excitation. In fact, this peak appears because in the perpendicular geometry, the u/g symmetry does not exist and the $^2\Pi_g$ and $^2\Pi_u$ resonances are coupled. Figure 4(b) presents structures around 6 and 8 eV that are associated with the opening of the inelastic channels corresponding to the $1\pi_u^3\ 1\pi_g^3$ configurations,[8] they are indeed also present in Fig. 4(a).

Secondly in the case of the perpendicular geometry [Fig. 4(a)], a very strong peak appears at negative energies. This peak is absent in the case of the free molecule, where negative energy scattering cannot be defined; in the case of an adsorbed molecule, negative energies correspond to the metal hot electrons. This peak is located at the position of the $O_2^-(^2\pi_g)$ resonance. It corresponds to the usual shape of a resonant process; a more or less Lorentzian structure peaking at the resonance energy. The excitation probability at maximum is rather large, around 0.6 and 0.2 for the *a* and *b* states.

Figures 5(a) and 5(b) present the inelasticities for the parallel geometry. As discussed in Sec. III, the $O_2^-(^2\Pi_g)$ resonance splits into a symmetric and an antisymmetric components, which contribute in different ways to the excitation. Similarly, the degenerate states of the O_2 neutral molecule split into two components and the $a\ ^1\Delta_g$ state presents two components which are excited in different ways. For the positive energies, the *A* and *S* components of $O_2^-(^2\Pi_g)$ lead to almost identical contributions to the excitation; they are also very close to those found in the perpendicular geometry (for this comparison, one has to sum the inelasticities for the *A* and *S* components of the $a\ ^1\Delta_g$ in the parallel geometry). This corresponds well to the interpretation of the excitation process outlined above; the excitation process involves the far wings of the resonance where the time delay is very short; the excitation then does not depend on the lifetime of the resonance (defined at the resonance center) and the various inelasticities are almost the same for the different geometries and for the free molecule. For the negative energies, the parallel geometry case also exhibits a peak at the resonance position. The interpretation is then that of a usual resonant process, occurring at the resonance center where the time delay is important and plays a role. The value of the excitation probabilities at the resonance position are directly linked to the partial widths of the $O_2^-(^2\Pi_g)$ resonance corresponding to the initial and outgoing channels. The partial width in a given channel depends on the tunneling rate of the electron at the channel energy and on the channel fractional parentage coefficient. As seen in Sec. III, the antisymmetric component of the $d\pi_g$ orbital is less coupled to the surface than the symmetric one and thus leads to a smaller partial width. This argument explains the relative magnitude of the various excitation probabilities in Figs. 4 and 5. As an example, let us consider the excitation of the $a\ ^1\Delta_g$ components in Fig. 5(b) (*A* component of the $^2\Pi_g$ resonance); since the resonant intermediate is *A*, the excitation of the *A* (resp *S*) component of the *a* state will involve the *S* (resp *A*) component of the $d\pi_g$ orbital; this predicts an excitation probability larger for the *A* component of the *a* state than for the *S* component, which is what can be seen in Fig. 5(b).

The above discussion separates the cases of negative and positive energies, i.e., of processes occurring around the resonance center or in the far wings of the resonance. Indeed, there exists an intermediate region where one goes from one situation to the other.

The present study is performed with the target molecule nuclei held fixed, i.e., assuming that the collision is so fast that the nuclei cannot move during the interaction. This approximation is perfectly valid in the far wings of the resonance where the collision is very fast; this is the case for the positive energies in Figs. 4 and 5. The electronic excitation probabilities are then obtained as averages of the probabilities computed with fixed nuclei over the distribution of internuclear distances; some vibrational excitation associated to the electronic excitation can also appear.[38] In the cases where the collision time is longer than or comparable to the target molecule vibrational frequency, then the study should be made including the vibration and an expansion over vibrational levels should be included in Ref. 2. In the present study with an adsorption height of $5a_0$, the width of the $O_2^-(^2\Pi_g)$ for the O_2 equilibrium distance varies between 0.07 eV and 0.15 eV depending on the symmetry and geometry,

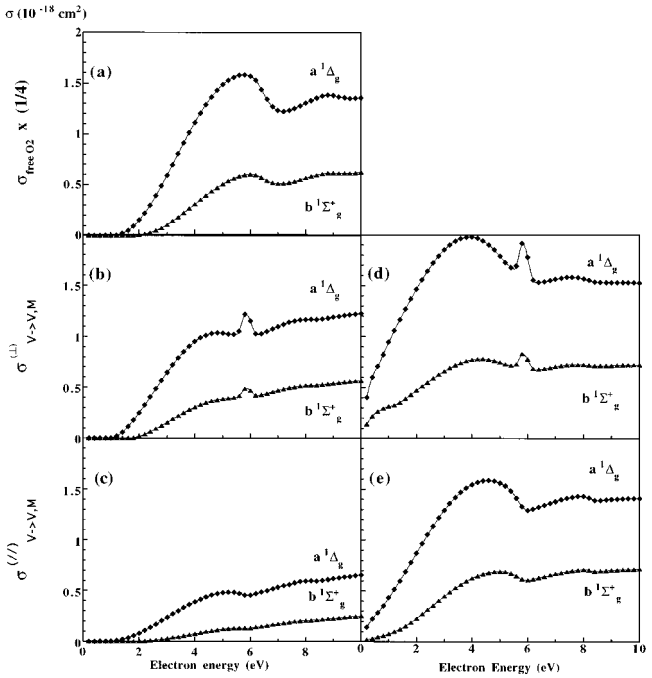

FIG. 6. Summed excitation cross sections for electron impact excitation of adsorbed O_2 molecules as functions of the incident electron energy. Diamonds, $a\ ^1\Delta_g$ state; triangles, $b\ ^1\Sigma_g^+$ state. (a) Free molecule; (b) *VV* process (see text) for the perpendicular geometry; (c) *VV* process (see text) for the parallel geometry; (d) *VM* process (see text) for the perpendicular geometry; (e) *VM* process (see text) for the parallel geometry.

i.e., it is of the order of magnitude of the O_2 vibrational quantum. The present results for the inelasticities at negative energies should then only be considered as estimates of the importance of this resonant process. A better treatment including the vibrational motion would lead to a resonant peak much broader in energy and possibly exhibiting an oscillating structure (see, e.g., Refs. 21–23).

C. Summed cross sections

Figure 6 presents the $(^2\Pi_g)$ resonant contributions to the *a* and *b* excitation cross sections as functions of the incident electron energy for three cases; the free molecule (*a*) and the molecule adsorbed in the perpendicular (*b* and *d*) and parallel (*c* and *e*) geometries. For the free molecule, the total excitation cross sections have been divided by 4, to allow a more direct comparison to the summed cross sections which are presented in the adsorbed molecule case (*VV* and *VM* cases). In the parallel geometry case, the excitation cross sections for the two components of the $a\ ^1\Delta_g$ state have been added.

The summed cross sections concern the *VV* and *VM* processes, i.e., the ones present in a scattering experiment; they only concern the positive energies, and the part of the resonant process occurring in the resonance wing. In this range, the inelasticities are very similar, however some differences appear between the summed cross sections, due to the classical sharing factors associated with the $V-M$ sharing (see Sec. IV and Ref. 22). The $g_{V,M}$ factors depend on the geometry and on the symmetry of the problem. From Fig. 3, one can see that in the parallel geometry the antisymmetric component of the resonant $d\pi$ orbital lies parallel to the surface, in contrast with the symmetric component. As a consequence, the g_V factor will be smaller in the case of an antisymmetric $(d\pi)$ component than for the symmetric component. The perpendicular geometry case behaves as the symmetric case in the parallel geometry. This feature explains the differences between the various summed cross sections.

As a striking feature, the order of magnitude of the various cross sections is not much different in the three cases and so, one can conclude that in a scattering experiment on adsorbed molecules, the resonant process involving the $(^2\Pi_g)$ O_2^- resonance will contribute in a way similar to the case of the free molecule, i.e., dominating for the lowest energies and yielding the bulk of the excitation cross sections on top of which other resonances contribute as peaks. As another feature, the *VM* process (incident electron from the vacuum, outgoing electron going into the metal) dominates over the *VV* process (both incident and outgoing electrons in the vacuum), however in a rather moderate way, except at very low energies. Indeed, for very low energies below the *a* or *b* excitation thresholds, the *VM* process is still possible whereas the *VV* process is impossible. These features are very different from the case of the vibrational excitations of N_2 via the $N_2^-(^2\Pi_g)$ resonance,[21–23] where the order of magnitude of the excitation cross sections was much smaller in the adsorbed case than in the free molecule and where the *VM* process was much stronger than the *VV* process, these two features being stronger for the excitation of the higher vibrational levels. This can be attributed to two effects; first, in the present case, the excitation involves the high energy wing of the resonance and is thus not much sensitive to the lifetime of the resonance i.e., to the adsorption; secondly, in the few eV range that is studied, the angular sharing, although important, does not introduce a very large weakening factor for the *V* side, in contrast with the lower energies involved in our previous study of e^--N_2 collisions.

The present results only concern the resonant $^2\Pi_g$ contribution to the excitation of the *a* and *b* states. It is expected to dominate this excitation in the low energy domain and to yield a background for the high energies. This makes difficult a quantitative comparison with the results of Ref. 27 on O_2/Ag(110) which concentrate on the high energy region and consider differential cross sections for given angles and not summed cross sections. However, in the O_2/Ag(110) system the O_2 molecular axis is oriented with respect to the Ag crystallographic axis and so an analysis of the angular distributions (polar and azimuthal angles) should bring informations on the resonant excitation mechanisms that could be compared with the present results (see below).

The above results on summed cross sections display differences between the various geometries although the excitation probabilities are very similar. In our calculation, this is entirely due to the differences between the shapes of the active resonant orbitals. The differences found on the values

of the summed cross sections should then be also visible on the angular distributions of the collisional electron (incident or outgoing), as functions of the polar or azimuthal angles. For the latter case, one needs a system in which the molecules are oriented in azimuth in a macroscopic way. As an example, the azimuthal angular distributions for the excitation of the $b\ ^1\Sigma_g^+$ state should be very different in the perpendicular and parallel geometries. In the perpendicular case, the distribution is isotropic; in the parallel case, one has two contributions corresponding to the two components of the $O_2^-(^2\Pi_g)$ resonance; the dominant one corresponds to the symmetric component of the resonance orbital and this should appear in the angular distribution which would then reflect the geometry of the system. However, it should be kept in mind that since the present work only considers the $(^2\Pi_g)$ resonance, the above angular discussion is restricted to the regions where the $(^2\Pi_g)$ resonance is dominant. In addition, possible multiple scattering effects cannot be ruled out.[39]

VI. CONCLUSIONS

Results have been presented on a theoretical study of the electronic excitation by low energy electron impact of O_2 molecules physisorbed on a model jellium metal surface (Al-like). The resonant contribution to this excitation involving the $O_2^-(^2\Pi_g)$ resonant intermediate has been considered; this resonant process provides the bulk of the excitation in the free molecule.

As the main results, in the case of a physisorbed molecule, the $O_2^-(^2\Pi_g)$ resonance contribute in an important way to the excitation of the spin forbidden $(X \rightarrow a\ ^1\Delta_g, X \rightarrow b\ ^1\Sigma_g^+)$ transitions, in a way very similar to that of the free molecule. In fact, this resonant process does not correspond to the usual picture of a resonant process, since it does not occur at the resonance position; it involves the high energy wing of the resonance, where the time delay is very small and then is almost not sensitive to the characteristics of the resonance. This feature should be rather general for all these resonant processes involving a resonant state hidden below the excitation threshold. In addition, the possibility for a physisorbed molecule to study electron impact at negative energy (i.e., below the vacuum level) reveals a new process with respect to the free molecule; the resonant excitation of O_2 at the resonance. In that case, the excitation probabilities are very large and much sensitive to the resonance characteristics i.e., to the symmetry and geometry of the problem. This excitation process should be present in situations with hot electrons.[40] The scattering results (as well as those involving hot electrons) depend on the symmetry and geometry of the problem, these dependences could only be revealed by studies of electron scattering by physisorbed molecules that analyze the angular distributions both in polar and azimuthal angles.

ACKNOWLEDGMENT

This work was supported by the Human Capital and Mobility programme of the European Community under Contract No. CHRX-CT93-0326.

[1] S. Trajmar and D. C. Cartwright, *Electron Molecule Collisions and Their Applications*, edited by L. G. Christophorou (Academic, New York, 1984), Vol. 1, pp. 155–249.
[2] F. Linder and Z. Schmidt, Z. Naturforsch **26A**, 1617 (1971).
[3] S. Trajmar, D. C. Cartwright, and W. Williams, Phys. Rev. A **4**, 1482 (1971).
[4] R. I. Hall and S. Trajmar, J. Phys. B **8**, L393 (1975).
[5] A. G. Middleton, P. J. O. Teubner, and M. J. Brunger, Phys. Rev. Lett. **69**, 2495 (1992).
[6] M. Allan, J. Phys. B **28**, 1 (1995).
[7] C. J. Noble and P. G. Burke, J. Phys. B **19**, L35 (1986).
[8] D. Teillet-Billy, L. Malegat, and J. P. Gauyacq, J. Phys. B **20**, 3201 (1987).
[9] D. Teillet-Billy, L. Malegat, and J. P. Gauyacq, J. Phys. B **22**, 1095 (1989).
[10] C. J. Noble, and P. G. Burke, Phys. Rev. Lett. **68**, 2011 (1992). K. Higgins, C. J. Noble, and P. G. Burke, J. Phys. B **27**, 3203 (1994).
[11] G. J. Schulz, Rev. Mod. Phys. **45**, 378 (1973).
[12] L. Sanche, J. Phys. B **23**, 1597 (1990).
[13] R. Palmer and P. Rous, Rev. Mod. Phys. **64**, 383 (1992).
[14] J. E. Demuth, D. Schmeisser, and Ph. Avouris, Phys. Rev. Lett. **47**, 1166 (1981).
[15] L. Sanche and M. Michaud, Phys. Rev. B **27**, 3856 (1983).
[16] K. Jacobi, C. Astaldi, P. Geng, and M. Bertolo, Surf. Sci. **223**, 569 (1989).
[17] J. W. Gadzuk, J. Chem. Phys. **79**, 3982 (1983).
[18] A. Gerber and A. Herzenberg, Phys. Rev. B **31**, 6219 (1985).
[19] D. Teillet-Billy, V. Djamo, and J. P. Gauyacq, Surf. Sci. **269/70**, 425 (1992).
[20] P. J. Rous, Surf. Sci. **260**, 361 (1992).
[21] V. Djamo, D. Teillet-Billy, and J. P. Gauyacq, Phys. Rev. Lett. **71**, 3267 (1993).
[22] V. Djamo, D. Teillet-Billy, and J. P. Gauyacq, Phys. Rev. B **51**, 5418 (1995).
[23] V. Djamo, D. Teillet-Billy, and J. P. Gauyacq, Surf. Sci. **346**, 253 (1996).
[24] D. Teillet-Billy, B. Bahrim, and J. P. Gauyacq, Nucl. Instrum. Methods B **100**, 296 (1995).
[25] E. T. Jensen, R. E. Palmer, and P. J. Rous, Surf. Sci. **237**, 153 (1990).
[26] J. C. Barnard, K. M. Hock, L. Siller, M. R. C. Hunt, J. F. Wendelken, and R. E. Palmer, Surf. Sci. **291**, 139 (1993).
[27] K. B. K. Tang and R. E. Palmer, Phys. Rev. B **53**, 1 (1996).
[28] E. S. Chang, J. Phys. B **10**, L677 (1977).
[29] V. Djamo, D. Teillet-Billy, and J. P. Gauyacq, in *Electron Scattering by Molecules, Clusters and Surfaces*, edited by L. Morgan and H. Ehrhardt (Plenum, New York, 1994), p. 217.
[30] D. Teillet-Billy and J. P. Gauyacq, Nucl. Instrum. Methods B **58**, 393 (1991).
[31] D. Teillet-Billy and J. P. Gauyacq, Surf. Sci. **239**, 343 (1990).
[32] P. J. Rous, Surf. Sci. Lett. **279**, L191 (1992).
[33] B. Bahrim, D. Teillet-Billy, and J. P. Gauyacq, Surf. Sci. **316**, 189 (1994).
[34] B. Bahrim, D. Teillet-Billy, and J. P. Gauyacq, Phys. Rev. B **50**, 7860 (1994).
[35] P. J. Jennings, R. O. Jones, and M. Weinert, Phys. Rev. B **37**, 6113 (1988).
[36] T. F. O'Malley, Phys. Rev. A **150**, 14 (1966).
[37] D. Teillet-Billy and J. P. Gauyacq, J. Phys. B **22**, L335 (1989).
[38] D. Teillet-Billy, J. P. Gauyacq, L. Malegat, R. Abouaf, and C. Benoit, Europhys. Lett. **6**, 139 (1988).
[39] E. T. Jensen, R. E. Palmer, and P. J. Rous, Surf. Sci. **237**, 153 (1990).
[40] F. Cemic, O. Dippel, K. W. Kolasinski, and E. Hasselbrink, Surf. Sci. **331/3**, 267 (1995); F. Cemic, O. Dippel, E. Hasselbrink, and R. Palmer, J. Chem. Soc. Faraday Trans **91**, 20 (1995).